

Toward Reconstructing Surfaces With Arbitrary Isotropic Reflectance : A Stratified Photometric Stereo Approach

Neil G. Alldrin

nalldrin@cs.ucsd.edu

David J. Kriegman

kriegman@cs.ucsd.edu

University of California, San Diego

Abstract

We consider the problem of reconstructing the shape of a surface with an arbitrary, spatially varying isotropic bidirectional reflectance distribution function (BRDF), and introduce a novel, stratified photometric stereo method. By using a particular configuration of lights, it is possible to use symmetry in the image measurements resulting from BRDF isotropy to estimate at each point a plane containing the surface normal. For differentiable surfaces, this allows us to recover the isocontours of the depth map, but not the actual depth associated with each contour. The isocontour structure provides topological information about the surface (critical points, Reeb graph, etc.). By using additional cues in the image data or imposing additional constraints on the surface (e.g., shadows, specular highlights, Helmholtz Reciprocity, uniform BRDF), the unknown height of each isocontour can be estimated and the metric structure is resolved. We validate this technique on real and synthetic data by successfully recovering the isocontours of the depth map from images.

1. Introduction

Reconstructing the shape of objects from images is one of the fundamental goals of computer vision. Because the problem is generally ill-posed, any solution will depend on some combination of constraints and prior knowledge which ultimately determine the performance of a given method. In photometric stereo the viewpoint is fixed and the illumination varies with each image; given strong enough constraints on object shape, illumination and/or the BRDF, surface normals and shape can be recovered.

Assuming distant (known) illumination and fixed viewpoint, one might wonder “What is the minimal set of constraints required to recover the shape of a surface?” To answer this question requires systematically defining the set of potential constraints and determining how each one restricts the surface shape. Figure 2 shows a hierarchy of pos-

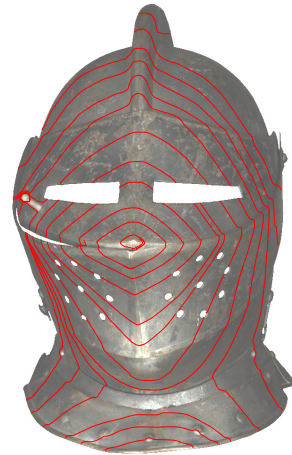


Figure 1: Isocontours of constant depth recovered by enforcing isotropy and surface differentiability.

sible constraints that could be employed in a photometric stereo setup to reconstruct a surface. In this paper we examine the cases of isotropic BRDF and surface smoothness / differentiability and show that just using isotropy, for every image point the surface normal can be constrained to a plane. By also imposing surface smoothness, the isocontour structure (e.g., curves of constant surface height) can be determined. While not a full Euclidean representation, the isocontour structure provides topological information about the surface (such as critical points and the Reeb graph) and could be sufficient for many applications including object recognition and parts inspection (for example, [18] uses iso-depth contours of human faces for face recognition). Moreover, by imposing any of the additional constraints listed in Figure 2 it is possible to recover the true surface barring degenerate cases. For example, at attached shadow boundaries the surface normal is constrained to lie in the plane orthogonal to the light source direction. Combined with isotropy this constrains the surface normal to lie in the intersection

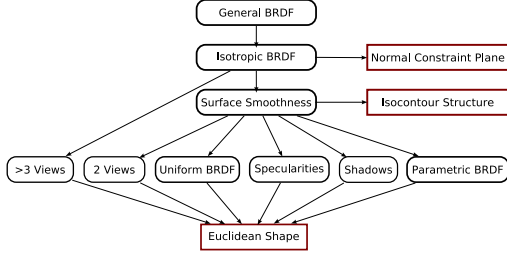


Figure 2: A hierarchy of assumptions whose corresponding constraints can be used to recover the surface of an object in a photometric stereo setup.

of two planes – a unique solution in general.

One of our main contributions is the use of a relatively unexplored physical property that holds for any isotropic BRDF – that isotropic BRDFs are symmetric about the plane spanned by the viewing direction and surface normal. From image data we show how to estimate this plane at each point and thus restrict the set of surface normals to lie in a plane. While we apply this constraint to photometric stereo, it could potentially be useful in other computer vision contexts as well.

2. Background and Related Work

Photometric stereo is a classic problem in computer vision first proposed by Woodham [24]. The basic idea is to infer the shape of an object by imaging it from a fixed viewpoint under varying illumination conditions. Early algorithms made strong assumptions on the reflectance function across the surface, typically requiring either explicit knowledge of the BRDF or simple parametric models, most often the Lambertian model.

A major thrust of more recent research has been to relax these assumptions to enable photometric stereo to work on broader classes of objects. For example, a whole line of research is based on the fact that the reflectance of many materials is well approximated by the sum of a specular lobe and a diffuse, Lambertian lobe [3, 1, 11, 16]. Coleman and Jain [3] and later Barsky and Petrou [1] (among others) assume the specular lobe has narrow angular extent, allowing them to perform Lambertian photometric stereo by treating specular pixels as outliers. Another approach is to exploit the dichromatic model under which the color of the specular lobe differs from the color of the diffuse lobe [21, 19, 14]. With knowledge of the light source color, this enables separation of the specular and diffuse components of the BRDF allowing Lambertian photometric stereo on the diffuse component.

Another approach, proposed by Hertzmann and Seitz [8, 9], is to use reference objects to essentially measure the

reflectance map for each lighting condition. This works for arbitrary BRDFs, but requires a reference object of the same material as the test object. Spatially varying BRDFs can also be handled in a limited way – this requires the BRDF of the test object to be closely approximated by the sum of a small number of basis BRDFs as well as reference objects whose BRDFs span the BRDFs present on the test object. More recently, Goldman et al. [7] removed the need for a reference object by iteratively estimating the basis BRDFs and surface normals. The downsides are that parametric BRDF models are reintroduced and convergence of the proposed optimization strategy seems non-trivial to achieve.

More similar to our approach are techniques that directly exploit various physical properties of BRDFs and illumination. For example, Helmholtz stereopsis [25, 26] exploits symmetry of the BRDF on the incident and exitant directions (i.e., Helmholtz reciprocity). Magda et al. [13] recover surface height using the squared distance intensity falloff of nearby light sources. Tan et al. [23] use both symmetry and reciprocity present in isotropic BRDFs to resolve the generalized bas-relief ambiguity.

3. The Bilateral Symmetry Constraint for Isotropic BRDFs

The crux of our algorithm is based on a known, but relatively unexplored property of isotropic BRDFs that has been previously referred to as *bilateral symmetry*¹ [15, 5]. Consider a surface patch with normal \mathbf{n} viewed from direction \mathbf{v} . Bilateral symmetry simply means that the BRDF is symmetric about the plane spanned by \mathbf{n} and \mathbf{v} with respect to the incident lighting direction \mathbf{s} (see Figure 3). Isotropic BRDFs are often described by the fact that the exitant radiance emitted from an isotropic surface patch is constant when the surface is rotated about its normal. Bilaterally symmetric BRDFs can similarly be described by the fact that the exitant radiance emitted from a bilaterally symmetric surface patch is constant when the surface is reflected about any plane colinear with its normal.

Looking again at Figure 3, consider some incident light source direction \mathbf{s} . Then there exists another direction \mathbf{s}' – obtained by reflecting \mathbf{s} about the plane spanned by \mathbf{n} and \mathbf{v} – that gives rise to the same reflectance. Following the notation of Tan et al. [23], we call such a pair of points an *isotropic pair*, which we define as,

Definition 1. *Two light source directions \mathbf{s} and \mathbf{s}' form an isotropic pair if they satisfy $\mathbf{n}^\top \mathbf{s} = \mathbf{n}^\top \mathbf{s}'$ and $\mathbf{v}^\top \mathbf{s} = \mathbf{v}^\top \mathbf{s}'$ where \mathbf{n} is the normal of a surface patch and \mathbf{v} is the viewing direction.*

¹Some authors consider isotropy and bilateral symmetry to be distinct phenomenon (i.e., isotropy $\not\Rightarrow$ bilateral symmetry); we do not make such a distinction since all or nearly all physically valid isotropic BRDFs have this property.

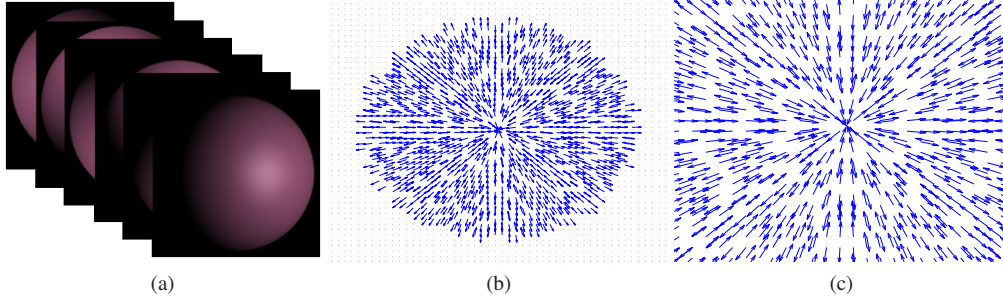


Figure 4: Surface gradient directions recovered from 36 images of a synthetic sphere. (a) Input images. (b) Quiver plot of gradient directions. (c) Zoom-in of quiver plot at center of sphere.

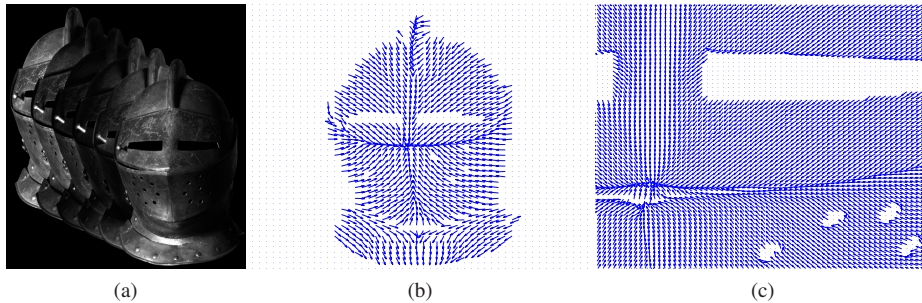


Figure 5: Surface gradient directions recovered from 32 images of a helmet. Note that the gradients have been flipped (if necessary) to point in the direction of maximum image intensity. (a) Input images. (b) Quiver plot of gradient directions. (c) Zoom-in of quiver plot near right eye.

the elevation angle θ so that,

$$\mathbf{s}_\theta(\phi) = (\sin \theta \cos \phi, \sin \theta \sin \phi, \cos \theta)^\top \quad (4)$$

which induces a 1D emitted radiance function,

$$E(\phi) = E(\mathbf{s}_\theta(\phi)). \quad (5)$$

This 1D radiance function is guaranteed to be symmetric² about angle ϕ_g , the azimuthal angle of the surface normal with respect to pole \mathbf{v} (or equivalently, the azimuthal angle of the surface gradient).

3.3. Symmetry Detection

In practice, we sample the emitted radiance function $E(\phi)$ at N uniformly spaced intervals and minimize the following objective to recover the symmetry angle ϕ_g at each pixel,

$$F(\phi_g) = \sum_{i=0}^{N-1} \min \left\{ \eta; \frac{E(\phi_i)}{E(r(\phi_i, \phi_g))} + \frac{E(r(\phi_i, \phi_g))}{E(\phi_i)} \right\}, \quad (6)$$

²Ignoring non-local illumination effects; such effects are handled in practice by treating them as outliers.

where η is a threshold to account for outliers and $r(\phi_i, \phi_g)$ is a function mapping angle ϕ_i to its reflected position about angle ϕ_g . In our experiments, we use a threshold of either $\eta = 2.1$ or $\eta = 2.2$. As for the number of samples N , this is clearly related to the angular frequency of $E(\phi)$; for the materials in our experiments we found that 20 to 30 samples are sufficient for accurate reconstruction. It should also be noted that this objective is robust to outliers, caused for example by cast shadows and interreflections. Moreover, attached shadows actually preserve symmetry and thus do not violate our assumptions in Section 3.1.

Figures 4 and 5 demonstrate our ability to recover the gradient direction using this approach. The sphere dataset consists of 36 images rendered in POV-Ray with source directions separated by 10° [17]. The helmet dataset consists of 32 images interpolated from a total set of 252 images taken about the sphere of lighting directions³; this corresponds to about 11° between light sources. In Figure 4, we see that the recovered gradient directions correctly point either toward or away from the center of the sphere. Figure 5 shows the recovered surface gradient directions for a hel-

³Data obtained from the Light Stage Data Gallery, ICT Graphics Lab, USC [4, 2].

met. While we do not have ground truth for this dataset, the gradients certainly seem plausible. It should be noted that symmetry is computed per-pixel, and thus our results are completely local.

4. Can Surface Constraints Resolve the Surface?

Based on the image acquisition setup described in Section 3.3, image measurements do not uniquely determine the surface normal, but constrain the surface normal to a plane. This is similar to shape from shading [10] where an image measurement constrains the normal to a cone, but does not fully determine the normal. In terms of the gradient of the height function, measurements provide the direction of the gradient, but not its magnitude. Here, we show that there is a family of surfaces that give rise to the same gradient direction at each surface point; thus surface constraints alone are insufficient to recover the full surface normal map. Yet, we show that for differentiable surfaces the isocontour structure can be recovered using only knowledge of the gradient direction.

4.1. A Class of Ambiguous Surfaces

Fact 4. Consider two surfaces given by height functions $z = f(x, y)$ and $z' = g(x, y)$ with gradient fields ∇f and ∇g respectively. Then the two surfaces have the same gradient direction if

$$\nabla g = k(x, y)\nabla f, \tag{7}$$

where $k(x, y)$ is some function of x and y that satisfies

$$\frac{\partial k}{\partial x} \frac{\partial f}{\partial x} = \frac{\partial k}{\partial y} \frac{\partial f}{\partial y} \tag{8}$$

for integrability to hold.

While we have not directly solved this system of partial differentiable equations, we do show the existence of a family of ambiguous surfaces,

Fact 5. Two surfaces defined by $z = f(x, y)$ and $z' = h(z)$ will have the same gradient direction at each point if h is a differentiable function of z .

Proof. This follows directly from Fact 4 and the chain rule,

$$\nabla h = \frac{\partial h}{\partial f} \nabla f \tag{9}$$

with $k(x, y) = \frac{\partial h}{\partial f}$. □

This implies that without additional information or constraints, we can at best recover a surface up to an arbitrary function of the true height. Figure 6 shows a set of surfaces with the same gradient direction at each point to illustrate this ambiguity.

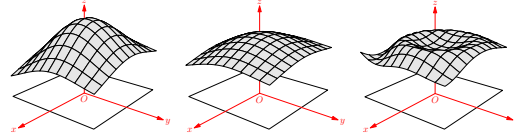


Figure 6: Three surfaces with the same gradient direction at each point.

4.2. Gradient Direction Resolves Isocontour Structure

We now show that two surfaces with the same gradient direction at each point must have height functions that result in the same set of iso-depth contour curves,

Theorem 1. Two surfaces defined by height functions $z = f(x, y)$ and $z' = g(x, y)$ that have the same gradient direction at each point must have the same set of iso-depth contour curves (i.e., curves of constant height).

Proof. Suppose $(x(t), y(t))$ corresponds to an iso-depth contour curve of z . Then $z(t) = f(x(t), y(t))$ and the derivative of z with respect to t is,

$$\frac{\partial z}{\partial t} = \frac{\partial f}{\partial x} \frac{\partial x}{\partial t} + \frac{\partial f}{\partial y} \frac{\partial y}{\partial t}. \tag{10}$$

Likewise, the derivative of z' with respect to t is,

$$\frac{\partial z'}{\partial t} = \frac{\partial g}{\partial x} \frac{\partial x}{\partial t} + \frac{\partial g}{\partial y} \frac{\partial y}{\partial t} \tag{11}$$

$$\frac{\partial z'}{\partial t} = k(t) \left(\frac{\partial f}{\partial x} \frac{\partial x}{\partial t} + \frac{\partial f}{\partial y} \frac{\partial y}{\partial t} \right) \tag{12}$$

$$\frac{\partial z'}{\partial t} = k(t) \frac{\partial z}{\partial t}, \tag{13}$$

where Equation 12 holds from Fact 4 since z and z' have the same gradient direction at each point. Now note that $\frac{\partial z}{\partial t} = 0$ since $(x(t), y(t))$ is an iso-depth curve of z ; combined with Equation 13 it is clear that $\frac{\partial z'}{\partial t} = 0$ meaning $(x(t), y(t))$ is an isocontour curve of z' as well. □

Theorem 1 tells us that an isocontour of the true surface height must be an isocontour of any surface height function that has the same set of gradient directions. This is quite significant because it reduces the problem of finding the true height at every surface point to the problem of finding the true surface height of a single point on each isocontour curve. Another consequence of Theorem 1 is that it is possible to recover iso-depth contours of a surface given only the direction of the gradient at each point – the tangent of the iso-depth contour at a given point is orthogonal to the direction of the gradient. Thus, it is possible to obtain iso-depth contour curves by tracing in the direction orthogonal to the gradient.

It is also important to note that Theorem 1 does not imply that the only class of ambiguous surfaces are functions of the true height (e.g., Fact 5). For example, consider two surfaces : one composed of two non-intersecting hemispheres and another composed of the same hemispheres with one of the hemispheres raised higher than the other. The two surfaces have the same gradient direction at each point and share the same iso-depth contours; however, the second surface is not a function of the first surface’s height.

4.3. Experimental Validation

To validate Theorem 1, we ran experiments on four datasets. For each surface shown in Figure 7 we first computed the gradient direction at each pixel as explained in Section 3.3. We then hand-selected a set of points on each surface and traced the iso-contour curves for some distance (~ 500 pixels) starting at those points. Clearly the iso-contour structure for the synthetic data closely matches the ground-truth. Also, while the true surface for the helmet is unknown, the iso-contour curves look highly plausible, with the exception of regions with depth discontinuities (such as the ridge on the helmet) which violate our assumption of surface differentiability. Figure 8 shows results on a knight. This is a much more challenging dataset, yet we still obtain reasonable results for most of the surface.

5. Recovering the Full Euclidean Structure

Suppose we have recovered the direction of the gradient at each point as well as the iso-depth contours of a surface, but do not know the true height of the surface nor the remaining component of the surface normals. As suggested in the introduction, to recover Euclidean structure we need to impose additional constraints (see Figure 2). Our options include (1) cast and attached shadows, (2) spatially uniform BRDF, (3) specularities, (4) multiple viewpoints, (5) parametric BRDF, (6) additional surface constraints, (7) structured lighting, and (8) heuristics [6]. Each of these constraints have previously been used in some form or another for surface reconstruction, but we have a distinct advantage since our surface is already highly constrained. In theory we only need to estimate a single value per iso-depth contour. In the following subsections we outline how one might fully constrain the surface by utilizing some of these constraints.

5.1. Shadow Constraints

Resolving structure from cast and attached shadows has been studied in some detail in the computer vision literature. Representative works include Shafer and Kanade [22] who first describe the constraints that shadow boundaries impose on a surface; Kriegman and Belhumeur [12] who show that the set of shadows produced by distant illumination can resolve the shape of a surface up to a generalized bas-relief

transformation when the lighting is unknown, and Savarese et al. [20] who implement a “shadow carving” algorithm.

The following facts capture the fundamental constraints that shadows provide,

Fact 6. *Consider a surface point that lies on an attached shadow boundary. Then the surface normal at that point must be orthogonal to the light source direction.*

Fact 7. *Consider a surface point \mathbf{p}_1 that lies on a shadow boundary cast by point \mathbf{p}_2 . Then the difference in height between the two points can be determined from the light source direction.*

Fact 6 suggests that the surface normal can be fully determined at the intersection of attached shadow boundaries and Fact 7 implies that surface height can be determined between cast shadow boundaries and corresponding occluding points (which are themselves attached shadow boundaries). A major hurdle to utilizing these facts is that detecting attached shadows is difficult to do reliably. However, if the iso-depth contours of the surface are known then constraints from noisy estimates of attached shadow boundaries can be distributed across entire isocontours, making the final surface estimate much more reliable than using shadows alone.

5.2. Uniform BRDF

If every surface point has the same BRDF then we can impose at least two additional constraints : constant brightness and reciprocity. The constant brightness constraint simply reflects the fact that points illuminated from the same light source direction will have the same intensity. Since we know the orientation of the surface normals and have measurements over a set of light source positions, we can effectively cluster the surface points according to the angle between the surface normal and viewing direction, $\mathbf{n}^\top \mathbf{v}$.

Helmholtz reciprocity imposes another set of constraints on the surface. Specifically, consider two surface points with surface normals \mathbf{n} and \mathbf{m} respectively. \mathbf{n} and \mathbf{m} are said to be reciprocal pairs under light source positions \mathbf{s}_n and \mathbf{s}_m if $\mathbf{n}^\top \mathbf{v} = \mathbf{m}^\top \mathbf{s}_m$ and $\mathbf{m}^\top \mathbf{v} = \mathbf{n}^\top \mathbf{s}_n$. It is well known that BRDFs which satisfy Helmholtz reciprocity are constant with respect to a reciprocal pair which means the image intensities corresponding to a reciprocal pair must satisfy,

$$E_n \mathbf{n}^\top \mathbf{v} = E_m \mathbf{m}^\top \mathbf{v}. \quad (14)$$

The problem then becomes one of isolating reciprocal pairs.

5.3. Specular Highlights

If we assume that the BRDF has a relatively tight specular lobe and that the specular lobe points in the idealized

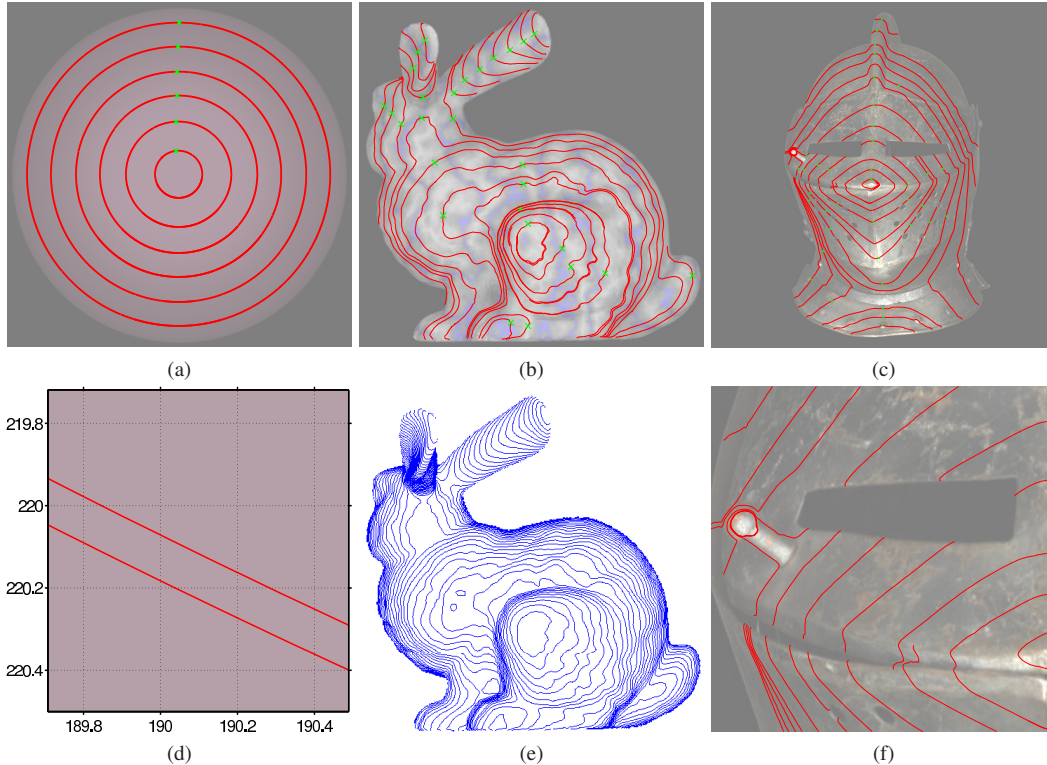


Figure 7: Recovered isocontour structure for three different data sets. (a) Synthetic sphere. (b) Synthetic bunny. (c) Helmet. (d) Zoom-in of inner-most isocontour. Notice the accumulated error after one loop is around 1/10th of a pixel. (e) Ground-truth isocontour map for the Stanford bunny. (f) Zoom-in of recovered isocontours on helmet.

reflection direction, then we can directly recover the surface normal at positions corresponding to specular peaks. Consider a surface point that coincides with a specular peak from light source direction \mathbf{s} . Then the surface normal at that point is given by the half angle between the viewing and source directions,

$$\mathbf{n} = (\mathbf{s} + \mathbf{v}) / \|\mathbf{s} + \mathbf{v}\|. \quad (15)$$

6. Conclusions and Future Work

Reconstructing shape from images is of fundamental importance to computer vision, yet is a very challenging problem that requires many constraints to effectively solve in practice. An unfortunate consequence is that many of the constraints used for shape reconstruction are only physically valid for very limited types of objects, or are not physically valid at all (e.g., brightness constancy in structure from motion). In this paper, we have shown how to utilize a relatively unexplored constraint for photometric stereo that is valid for arbitrary, unknown, and spatially varying isotropic materials. Much like Helmholtz reciprocity, bilateral symmetry is an important physical property of isotropic BRDFs that can and should be utilized when possible. Unlike most

competing methods, we do not assume any parametric form for the BRDF, making our technique the least restrictive to date with respect to assumptions on object reflectance.

While bilateral symmetry is only strong enough to constrain the surface normal at each point to a plane, we show how additional assumptions can be used to recover further structure. A particularly interesting case is surface differentiability which, when combined with bilateral symmetry, constrains the surface up to a set of iso-depth contour curves. This representation, which has been shown to be useful in its own right [18], reveals object topology (singular points and saddle points stand out for example) and reduces the surface ambiguity to a single value per iso-depth contour. The use of further constraints to fully resolve Euclidean structure is left to future work.

Acknowledgements

This work was partially funded under NSF grants IIS-0308185 and EIA-0303622.

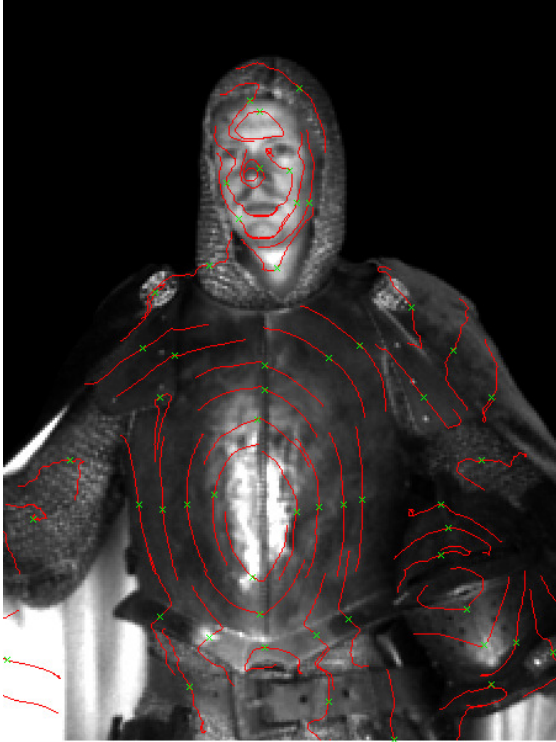


Figure 8: Recovered isocontour structure of a knight [4, 2]. Note that some regions (e.g., chain-mail) violate our assumptions of isotropy and/or surface differentiability.

References

- [1] S. Barsky and M. Petrou. The 4-source photometric stereo technique for three-dimensional surfaces in the presence of highlights and shadows. *IEEE Trans. on PAMI*, 25(10):1239–1252, 2003.
- [2] C.-F. Chabert et al. Relighting human locomotion with flowed reflectance fields. In *SIGGRAPH '06 (Sketches)*, page 76, 2006.
- [3] E. Coleman, Jr. and R. Jain. Obtaining 3-dimensional shape of textured and specular surfaces using four-source photometry. *CGIP '82*, 18(4):309–328, April 1982.
- [4] P. Debevec et al. Acquiring the reflectance field of a human face. In *SIGGRAPH '00*, pages 145–156, 2000.
- [5] O. Drbohlav. *Towards Uncalibrated Photometric Stereo for Non-Lambertian Surfaces*. PhD thesis, Czech Technical University, September 2003.
- [6] A. Ecker, K. Kutulakos, and A. Jepson. Shape from planar curves: A linear escape from flatland. In *CVPR '07*, pages 1–8, 2007.
- [7] D. Goldman et al. Shape and spatially-varying brdfs from photometric stereo. In *ICCV '05*, 2005.
- [8] A. Hertzmann and S. M. Seitz. Shape and materials by example: A photometric stereo approach. In *CVPR '03*, volume 01, page 533, 2003.
- [9] A. Hertzmann and S. M. Seitz. Example-based photometric stereo: Shape reconstruction with general, varying brdfs. *IEEE Trans. on PAMI*, 27(8):1254–1264, 2005.
- [10] B. Horn. *Shape from Shading: A Method for Obtaining the Shape of a Smooth Opaque Object from One View*. PhD thesis, MIT, 1970.
- [11] K. Ikeuchi. Determining surface orientations of specular surfaces by using the photometric stereo method. *IEEE Trans. on PAMI*, 3(6):661–669, November 1981.
- [12] D. Kriegman and P. Belhumeur. What shadows reveal about object structure. *J. Optical Soc. Am. A*, 18(8):1804–1813, 2001.
- [13] S. Magda et al. Beyond lambert: Reconstructing surfaces with arbitrary brdfs. In *ICCV '01*, volume 2, pages 391–398, 2001.
- [14] S. P. Mallick et al. Beyond lambert: Reconstructing specular surfaces using color. In *CVPR '05*, volume 2, pages 619–626, 2005.
- [15] S. R. Marschner. *Inverse Rendering for Computer Graphics*. PhD thesis, Cornell, 1998.
- [16] S. Nayar, K. Ikeuchi, and T. Kanade. Determining shape and reflectance of hybrid surfaces by photometric sampling. *IEEE Trans. on Robotics and Automation*, 6(4):418–431, August 1990.
- [17] POV-Ray – The Persistence of Vision Raytracer. A high-quality, totally free tool for creating stunning three-dimensional graphics. <http://www.povray.org>.
- [18] C. Samir, A. Srivastava, and M. Daoudi. Three-dimensional face recognition using shapes of facial curves. *IEEE Trans. on PAMI*, 28(11):1858–1862, 2006.
- [19] Y. Sato and K. Ikeuchi. Temporal-color space analysis of reflection. *J. Optical Soc. Am. A*, 11(11):2990–3002, November 1994.
- [20] S. Savarese et al. 3d reconstruction by shadow carving: Theory and practical evaluation. *IJCV '07*, 71(3):305–336, March 2007.
- [21] K. Schlüns and O. Wittig. Photometric stereo for non-lambertian surfaces using color information. In *Int. Conf. on Image Anal. and Proc.*, pages 505–512, September 1993.
- [22] S. Shafer and T. Kanade. Using shadows in finding surface orientations. *CVGIP '83*, 22:145–176, 1983.
- [23] P. Tan et al. Isotropy, reciprocity and the generalized bas-relief ambiguity. In *To appear in the Proc. of CVPR '07*, 2007.
- [24] R. Woodham. Photometric method for determining surface orientation from multiple images. *Optical Engineering*, 19(1):139–144, January 1980.
- [25] T. Zickler, P. N. Belhumeur, and D. J. Kriegman. Helmholtz stereopsis: Exploiting reciprocity for surface reconstruction. In *ECCV '02*, volume 3, pages 869–884, 2002.
- [26] T. E. Zickler, P. N. Belhumeur, and D. J. Kriegman. Helmholtz stereopsis: Exploiting reciprocity for surface reconstruction. *IJCV '02*, 49(2-3):215–227, 2002.